

## LATTICE DYNAMICS OF SILVER AND GOLD ON KREBS'S MODEL

BY L. A. BERTOLO\* AND M. M. SHUKLA\*\*

Instituto de Física "Gleb Wataghin", Universidade Estadual de Campinas

(Received May 5, 1978; final version received June 12, 1979)

Phonon dispersion relations along the principal symmetry directions of gold and silver have been calculated for phonons propagating at room temperature. The calculated curves are compared with the recent experimental findings. Also calculated are the lattice heat capacities of these metals at absolute zero temperature. Computed  $(\theta-T)$  curves of them show good agreements with experimental results. The effect of various forms of the dielectric screening functions on the calculated phonon spectrum of gold and silver has also been investigated.

### 1. Introduction

Krebs [1, 2] has propounded a phenomenological model for lattice dynamics of cubic metals. His model has achieved a profound success in interpreting the experimental phonon dispersion curves along the principal symmetry directions as well as the heat capacities of almost all cubic metals (see for example Krebs [1, 2], Shukla [3, 4], Shukla and Dayal [5-7], Mahesh and Dayal [8, 9] and S. Pal [10]). The success of Krebs's [1, 2] model for all the cubic metals was based on two aspects, namely, the application of central interionic interactions and the use of electron-ion interaction on a screened coulomb interaction which had preserved the lattice periodicity in the reciprocal space due to the use of umklapp process following the ingenious idea of Lax [11]. The experimental phonon dispersion curves of silver and gold have been determined quite recently. This gave us an opportunity to test the applicability of Krebs's model as far as the reproduction of experimental results were concerned. It was found that original Krebs's [1, 2] model did not reproduce the experimental results. We, thus, have considered interionic interactions out to third neighbours also. One more basic modification in the original model of Krebs [1, 2] was

---

\* Present address: Departamento de Física, Instituto de Ciências Exatas, Universidade Federal Rural do Rio de Janeiro, Km 47 do Antigo Rio-São Paulo, Rio de Janeiro, Brasil.

\*\* On leave from UNICAMP. Visiting Professor of the Department of Electrical Engineering, University of Rhode Island, Kingston, R. I. 02881, USA. Present address: Instituto de Física "Gleb Wataghin", Universidade Estadual de Campinas, C. P. 1170-13100 Campinas, SP Brasil.

made by replacing the dielectric screening function of Lindhardt to all other existing forms for such functions. This would give us an opportunity to test the effects of various dielectric screening functions in the calculations of the phonon frequencies of silver and gold. The existence of numerous experimental elastic and thermal data tempted us also to calculate and compare with experiments the lattice heat capacities of these two noble metals.

## 2. Theory

The frequency of vibration of monoatomic cubic solid can be obtained from the solution of the  $3 \times 3$  determinantal equation of the form

$$|D_{\alpha\beta}(q) - M\omega^2 I \delta_{\alpha\beta}| = 0, \quad (1)$$

where  $I$  is the unit matrix of order three and  $M$  is the mass of atom. Each element of the dynamical matrix  $D_{\alpha\beta}(q)$  is split up into two parts: the ion-ion interaction part  $D_{\alpha\beta}(q)$  and the electron-ion interaction part  $D_{\alpha\beta}^{ie}(q)$ . Written mathematically,

$$D_{\alpha\beta}(q) = D_{\alpha\beta}^{ii}(q) + D_{\alpha\beta}^{ie}(q). \quad (2)$$

By confining the ion-ion interactions up to third neighbours only, we get the explicit expression for a typical diagonal and non-diagonal element of the dynamical matrix.

$$D_{\alpha\alpha}^{ii}(q) = 2\alpha_1[2 - C_i(C_j + C_k)] + 4\alpha_2 S_i^2 + 8\alpha_3[2/3 C_j C_k (2C_i^2 - 1) - 1/6 C_i C_k (2C_j^2 - 1) - 1/6 C_i C_j (2C_k^2 - 1)], \quad (3)$$

$$D_{\alpha\beta}^{ii}(q) = 2\alpha_1 S_i S_j + 4/3 \alpha_3 [S_i S_j (2C_k^2 - 1) + 4C_k (C_i + C_j)]. \quad (4)$$

The electron-ion interaction is taken on of Krebs's [1, 2] model and a typical expression for the diagonal matrix describing such an interaction is given by

$$D_{\alpha\beta}^{ie}(q) = \frac{1}{4} a^3 \lambda^2 k_c \left[ \frac{(q_i + h_i)(q_j + h_j) G^2(\mu_1)}{|q + h|^2 + \frac{a^2 \lambda^2}{4\pi^2} f(t_1)} - \frac{h_i h_j G^2(\mu_2)}{h^2 + \frac{a^2 \lambda^2}{4\pi^2} f(t_2)} \right]. \quad (5)$$

In the above expressions  $\alpha_i$  are the force constants for the  $i$ -th neighbour.

$$S_i = \sin(\pi a k_i), \quad C_i = \cos(\pi a k_i), \quad q_i = \frac{a k_i}{2\pi},$$

$$\lambda = C \left( \frac{r_s}{a_B} \right)^{1/2} k_F, \quad 0.353 \leq C \leq 0.814, \quad g(\mu) = \frac{3(\sin \mu - \mu \cos \mu)}{\mu^3}, \quad (6)$$

$k_i (i = 1, 2, 3)$  are the cartesian components of the wave vector,  $h_i (i = 1, 2, 3)$  represent the cartesian components of the reciprocal lattice wave vector,  $a$  — the lattice parameter,

$k_F$  — the Fermi wave vector,  $r_s$  — the radius of the atomic sphere,  $a_B$  — the Bohr radius,  $k_e$  — the Bulk modulus of the electron gas.

The function  $f(t)$  is the dielectric screening function. Krebs [1, 2] has used the form given by Lindhardt [12]

$$f(t) = \frac{1}{2} + \frac{4-t^2}{8t} \ln \frac{2+t}{2-t}, \quad (7)$$

with

$$t_1 = \frac{\pi}{ak_F} |q+h| \quad \text{and} \quad t_2 = \frac{\pi}{ak_F} h.$$

We have introduced in the Krebs's formalism the other existing forms of the dielectric screening functions given by

$$f(t) = \frac{f(q)}{(1-F(t)f(q))}, \quad (8)$$

where

$$f(q) = \frac{1}{2} q^2 / (q^2 + k_F^2 + k_{TF}^2), \quad (9)$$

where  $k_{TF}$  is Thomas-Fermi radius vector. Another form of  $f(t)$  comes from the work of Geldert and Vosko [14], given by replacing  $f(q)$  in Eq. (8) by

$$f(q) = \frac{1}{2} \frac{q^2}{q^2 + \xi k_F^2}, \quad (10)$$

where

$$\xi = \frac{2}{1 + 0.026 r_s^*}, \quad (11)$$

where

$$r_s^* = \frac{m^*}{m} r_s, \quad (12)$$

$m$  and  $m^*$  are the mass and effective mass of electron. The Kleinman and Langreth [15] form of  $f(t)$  is obtained by replacing the  $f(q)$  in Eq. (8) by

$$f(q) = \frac{1}{4} \left( \frac{2}{q^2 + k_F^2 + k_s^2} + \frac{q^2}{k_F^2 + k_s^2} \right), \quad (13)$$

where  $k_s$  is the screening parameter expressible in the Nozières and Pines [16] interpolation scheme by

$$\frac{k_s^2}{k_F^2} = \frac{1 - 0.0395 \left( \frac{k_{TF}}{k_F} \right)^2}{1 + 0.0395 \left( \frac{k_{TF}}{k_F} \right)^2}. \quad (14)$$

Overhauser [17] has given another form of  $f(t)$  which can be obtained by replacing  $f(q)$  in Eq. (8) by the formula given below

$$f(q) = \frac{1.1x^2}{(1 + 10x^2 + 1.5x^4)^{1/2}}. \quad (15)$$

The  $f(t)$  functions given by Singwi et al. [17] can be obtained by replacing the  $f(q)$  in Eq. (8) by the expression given below

$$f(q) = A(1 - e^{-B(q/k_F)^2}). \quad (16)$$

By expanding the secular determinant in the longwavelength limit ( $q \rightarrow 0$ ), the following relations are obtained between the elastic constants and force constants

$$aC_{11} = 2\alpha_1 + 4\alpha_2 + 12\alpha_3 + aKe, \quad (17)$$

$$aC_{12} = \alpha_1 + 6\alpha_3 + aKe, \quad (18)$$

$$aC_{44} = \alpha_1 + 6\alpha_3. \quad (19)$$

### 3. Numerical computations

Before the phonon dispersion relations and lattice heat capacities are calculated, the evaluation of the free parameters of the model becomes necessary. There are four disposable parameters in the model. To evaluate them uniquely we have employed four equations, three between elastic constants and force constants and one between force constants and frequency from the boundary of Brillouin zone. Several choices were made for this frequency but finally longitudinal zone boundary from  $|\xi\xi\xi|$  directions was selected. In order to have a direct comparison with the experimental phonon relations, the phonon frequencies along symmetry directions were calculated by employing the other experimental data at the temperature at which experimental phonons were determined.

The phonon frequencies of silver were determined by Kamitakahara and Brockhouse [19] and that of gold by Lynn et al. [20] at room temperature only. Thus, elastic constants and lattice parameter were taken at the room temperature only. The experimental elastic

TABLE I

Input data to calculate force constants of silver and gold

Substance	Temperature [K]	Elastic constant in $10^{11}$ dyn $\text{cm}^{-2}$			Lattice parameter $\text{\AA}^\circ$	Phonon frequency $10^{12}\text{Hz}$
		$C_{11}$	$C_{12}$	$C_{44}$		
Silver	0	13.15	9.73	5.11	4.06	$\nu_{L.5.5.5} = 5.21$
	296	12.40	9.34	4.61	4.08	$\nu_{L.5.5.5} = 5.07$
Gold	0	20.16	16.97	4.54	4.056	$\nu_{L.1.0.0} = 4.69$
	296	19.23	16.31	4.20	4.070	$\nu_{L.1.0.0} = 4.61$

TABLE II

Force constants of silver at room temperature unit  $10^3$  dyn  $\text{cm}^{-1}$ 

Dielectric screening function	$\alpha$	$\beta$	$\gamma$	$ake$
Lindhardt	22.279	-1.1611	-.578	19.390
Modified Hubbard's form	22.740	-1.611	-.666	19.390
Klein and Langreth	22.291	-1.581	-.580	19.298
Vosko et al.	22.326	-1.611	-.586	19.390
Overhauser	21.177	-1.581	-.395	19.298

TABLE III

Force constants of gold at room temperature unit  $10^3$  dyn  $\text{cm}^{-1}$ 

Dielectric screening function	$\alpha$	$\beta$	$\gamma$	$ake$
Lindhardt	32.994	-1.292	-2.649	49.247
Modified Hubbard's form	33.491	-1.292	-2.732	49.247
Klein and Langreth	31.931	-1.302	-2.473	49.288
Vosko et al.	33.090	-1.292	-2.666	49.247
Overhauser	39.900	-1.302	-2.134	49.288

constants of silver and gold were taken from the measurement of Neighbours and Alers [21]. The input data to calculate atomic force constants are given in Table I. Output values of the force constants are presented in Tables II and III.

In figures 1 and 2 are shown the computed phonon dispersion curves of silver and gold along the principal symmetry directions. In those figures are also plotted the experimental frequencies for comparison purpose. While the theoretical curves are shown by continuous lines, experimental points are shown by different symbols given in the captions. The computed curves correspond to the dielectric functions used by Krebs [1, 2].

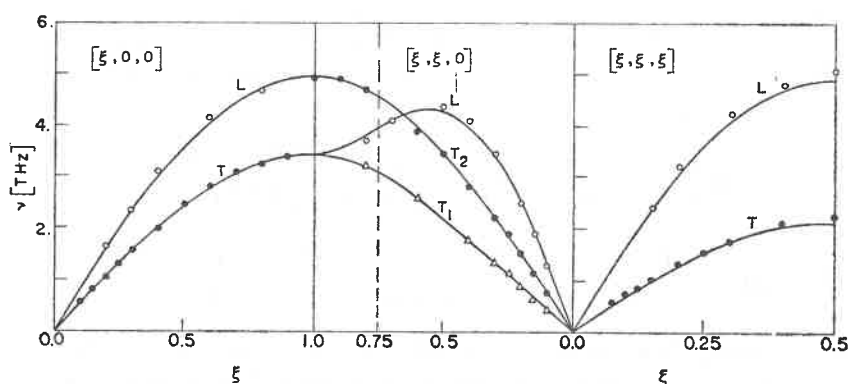


Fig. 1. Phonon dispersion curves of silver along the principal symmetry directions

We have also investigated the effect of introducing the various forms of the dielectric screening function on phonon frequencies of silver and gold. For that purpose we have tried all the various forms described in the theory except that of Singwi et al. [18] as we could not get the values of  $A$  and  $B$  appearing in the work of Singwi for silver and gold.

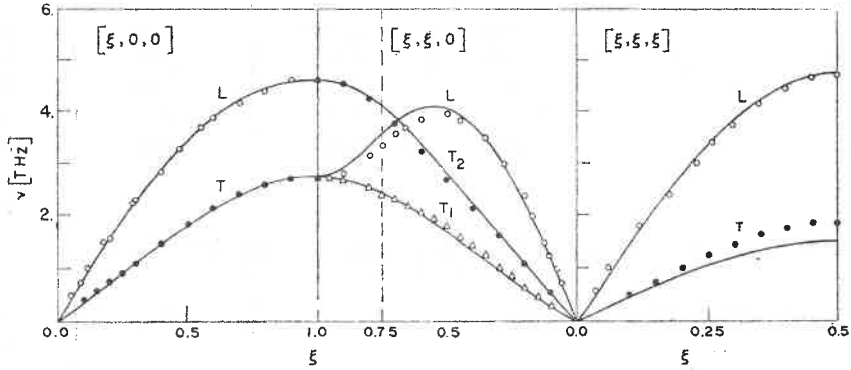


Fig. 2. Phonon dispersion relations in gold along the principal symmetry directions. Theoretical curves are shown by continuous lines. Experimental points from the measurements of Lynn et al. are shown by  $\circ$

Every time new dielectric screening function was employed with the same input data, we had obtained different sets of force constants. In Tables II and III are shown the output values of the force constants by using different dielectric screening functions. The phonon dispersion relations in silver and gold have been calculated with each set of force constants. It was observed that for low wave vectors all the sets of the force constants gave identical frequencies. The maximum deviation between one set of results to other was found to be about 1% near the high frequency ends. Thus all different sets of dispersion curves were not plotted. The figures 1 and 2 correspond to the usual Lindhardt's dielectric functions.

To calculate the lattice heat capacities of silver and gold, zero degree Kelvin values of the force constants were evaluated. For that purpose, we took the extrapolated values of elastic constants of silver and gold. The lattice constants of silver and gold at  $0^\circ$  Kelvin were extrapolated from the thermal expansion data of Behari and Tripathi [22]. The zero degree Kelvin values of phonon frequencies were extrapolated on the following scheme based on the work of Varshni and Yuen [23].

$$v_{L\xi\xi\xi} : \frac{v_b(^{\circ}\text{K})}{v_b(296^{\circ}\text{K})} = \left[ \frac{(C_{11})^{\circ}\text{K} a^3(^{\circ}\text{K})}{(C_{11})296^{\circ}\text{K} a^3(296^{\circ}\text{K})} \right]^{1/2}$$

$$v_{L\xi 00} : \frac{v_b(^{\circ}\text{K})}{v_b(296^{\circ}\text{K})} = \left[ \frac{(C_{11} + 2C_{12} + 4C_{44})^{\circ}\text{K} a^3(^{\circ}\text{K})}{(C_{11} + 2C_{12} + 4C_{44})296^{\circ}\text{K} a^3(296^{\circ}\text{K})} \right]^{1/2}$$

The input data to calculate atomic force constant at zero degree Kelvin are given in Table I. The output values of atomic force constants for silver and gold at zero degree Kelvin temperature using different dielectric screening functions are given in Tables IV and V.

TABLE IV

Force constants of silver at zero degree Kelvin temperature unit  $10^3$  dyn  $\text{cm}^{-1}$ 

Dielectric screening function	$\alpha$	$\beta$	$\gamma$	$ake$
Lindhardt	20.166	-1.715	-.097	18.757
Modified Hubbard's form	21.126	-1.715	-.046	18.757
Klein and Langreth	22.159	-1.715	-.023	18.757
Vosko et al.	20.257	-1.715	-.081	18.757
Overhauser	21.086	-1.715	-.057	18.757

TABLE V

Force constants of gold at zero degree Kelvin temperature unit  $10^3$  dyn  $\text{cm}^{-1}$ 

Dielectric screening function	$\alpha$	$\beta$	$\gamma$	$ake$
Lindhardt	28.659	-1.370	-1.707	50.416
Modified Hubbard's form	29.602	-1.370	-1.864	50.461
Klein and Langreth	32.052	-1.370	-2.273	50.416
Vosko et al.	28.823	-1.370	-1.735	50.416
Overhauser	29.587	-1.370	-1.862	50.416

In order to calculate lattice heat capacities we have divided the first Brillouin zone into an equally spaced wavevector space in 8000 parts. The lattice periodicity made it possible to calculate the frequencies only for 262 non equivalent points including the origin. The resulting phonon spectra were utilized to plot  $g(\nu)$  versus  $\nu$  curve to calculate  $C_v$  on Blackman's Sampling Technique. The resultant  $C_v$  was utilized to calculate  $\theta$ .

We have calculated  $(\theta - T)$  curves of silver and gold by using all five different values of atomic force constants given in Tables IV and V. The different resultant  $(\theta - T)$  curves of silver and gold did not differ much from each other. We, thus, have plotted in figures 3 and 4 the  $(\theta - T)$  curves of silver and gold using the dielectric screening function of Lindhardt [12] only. In those figures are also plotted the experimental  $(\theta - T)$  curves of silver and gold. The experimental  $C_v$  of silver and gold have been taken respectively from the work of Giaque and Meads [24] and that of Frebelle and Giaque [25]. To estimate the lattice heat capacities of these metals, the electronic specific heat part,  $\gamma$ , was taken to be equal to 0.65 and 0.74 in units of  $\text{mJ mol}^{-1} \text{deg}^{-2}$  respectively for silver and gold from the measurements of Yates and Hoare [26] and that of Corek et al. [27].

A critical study of figure 1 reveals the fact that the calculated phonon dispersion curves of silver along all the three principle symmetry directions have reproduced extremely well the experimental results. Except at few wave vectors in the high frequency ends for some of branches of the dispersion curves, the calculated curves have reproduced the experimental ones within the limits of the experimental errors. The maximum deviations found between the calculated and experimental phonon are found to be of the order of 6%.

A study of figure 3 reveals the information that the calculated  $(\theta-T)$  curve of silver has reproduced the entire course of the experimental results and is found to lie about 2% above the experimental curve.

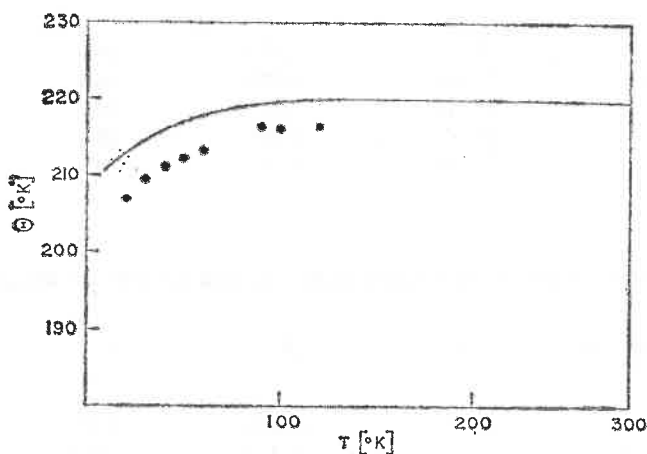


Fig. 3.  $(\theta-T)$  curves of silver. Continuous line shows the theoretical curve. Experimental points are shown by ●

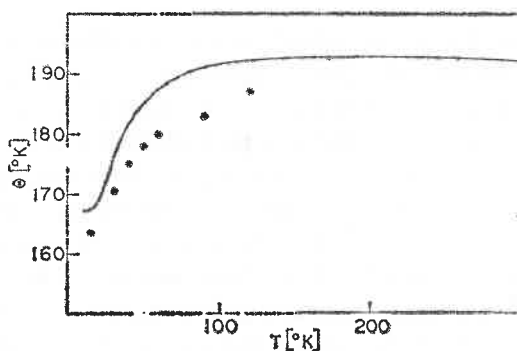


Fig. 4.  $(\theta-T)$  curves of gold. Continuous line shows the theoretical curve. Experimental points are shown by ●

A critical survey of figure 2 indicates that the calculated phonon dispersion curves of gold have reproduced extremely well the experimental results of Lynn et al. [20] along all the three principal symmetry directions. At low wave vectors the calculated curves have reproduced the experimental results. A little deviation exists between the two sets of results in the transverse branches of  $|\xi\xi\xi|$  and  $|\xi\xi 0|$  directions. But, in every case, the experimental phonons are found to differ from the theoretical results only by 6%.

A critical study of figure 4 reveals the fact that the calculated  $(\theta-T)$  curve of gold has reproduced the entire course for the experimental curve and lies about 2% below it.



#### 4. Discussion and conclusion

The present study of the lattice dynamics and heat capacities of silver and gold on Krebs's model have shown that the computed phonon dispersion curves as well  $(\theta-T)$  curves show an excellent agreement with the experimental results. The maximum departure between the calculated and experimental frequency is found to be less than 6% and for the case of  $\theta$  less than 2%.

It is worthwhile to compare present results with the other existing theoretical computations. Kamitakahara and Brockhouse [19] have employed as many as 12 parameters in their point ion model study to fit the experimental phonon dispersion relations in silver. Lynn et al. [20] had to employ as many as 16 parameters to fit their experimental phonon dispersion curves of gold. Even with using such a huge number of parameters in their point ion model studies these authors could not fit their experimental phonon dispersion curves better than those given by the present results. It is just an obvious fact as these authors have ignored the electron-ion interaction in metals. This is the basic reason why they could not fit  $q \rightarrow 0$  limit results i.e. the experimental elastic constants also.

The earlier study of lattice dynamics of silver and gold by Shukla [4] and Shukla and Dayal [5] is quite inferior to the present result. The numerical values of the force constants given by these authors could not explain very well the phonon dispersion relations in these metals. In the absence of the experimental phonon dispersion relations in gold and silver, Shukla and Dayal [7] have tried to fit the experimental  $(\theta-T)$  curves of them. In doing that they drew a false conclusion that electron screening in noble metals varied in between the limits predicted by the theories of Bohm and Pines and Thomas and Fermi. Where as we found that electron screening in silver and gold is governed only by the theory of Bohm and Pines. This result is in confirmation with the recent result of Closs and Shukla [28]. The only change found necessary, in Krebs's model to interpret experimental phonon dispersion relations was to include the interionic interactions out to third neighbour.

We also investigated the effect of the introduction of the various forms of the dielectric screening functions in Krebs's model as far as the evaluation of phonon frequencies of silver and gold were concerned. A critical study of Tables II and III would show that the atomic force constants of silver and gold varied very little with the use of the different dielectric screening function.

The entire phonon spectrum of them did not differ from each other more than 1% when the individual frequencies were compared from the different dielectric screening functions. This kind of result is a little bit surprising when compared with the results on models on first principles (see Price et al. [29]) where the different dielectric screening functions have got drastic influences on the computed phonon frequencies of simple metals. Two conclusions could be derived from the present results. Firstly, for monovalents metal (silver and gold) different dielectric screening functions have got very little effect in the computation of phonon frequencies. Secondly, the individual effect of the dielectric function is lost in the evaluation of the phonon frequencies. This is because the introduction of the bulk modulus of electron gas in Krebs's model is only on an empirical basis i.e.  $q \rightarrow 0$  limit. Probably, a best test of the effect of the dielectric screening

function would be to employ the model of Krebs and Holtz [30]. A remark about the evaluation of  $\theta$  should be made. The  $\theta$  represents a statistical parameter of the model which is obtained by an averaging over the entire phonon spectrum. Thus, how so ever good a model may be in interpreting the experimental phonon dispersion curves along the principal symmetry directions, it would never predict extremely well the  $(\theta-T)$  curve. These two properties are independent checks of the model. No doubt, a good fit with experimental phonon dispersion curves ensures a good agreement with the experimental  $(\theta-T)$  curve but reverse is not true.

The authors thank Dr. R. C. C. Leite, Dean of the faculties of UNICAMP, for providing the necessary research facilities. One of us (L. A. Bertolo) also acknowledges the fellowships support from FAPESP. This work was also partially supported by BNDE, FNDCT, CNPq and BADESP. Computational help from Mr. Antonio Assis Leite Filho as well computational facilities from UNICAMP computer centre is also acknowledged.

#### REFERENCES

- [1] K. Krebs, *Phys. Lett.* **10**, 12 (1964).
- [2] K. Krebs, *Phys. Rev.* **138**, A143 (1965).
- [3] M. M. Shukla, *Phys. Status Solidi* **7**, K11 (1964).
- [4] M. M. Shukla, *Phys. Status Solidi* **8**, 485 (1965).
- [5] M. M. Shukla, B. Dayal, *Phys. Status Solidi* **16**, 513 (1966).
- [6] M. M. Shukla, B. Dayal, *Phys. Status Solidi* **19**, 729 (1967).
- [7] M. M. Shukla, B. Dayal, *J. Phys. Chem. Solids* **26**, 1343 (1965).
- [8] P. S. Mahesh, B. Dayal, *Phys. Status Solidi* **9**, 351 (1965).
- [9] P. S. Mahesh, B. Dayal, *Phys. Rev.* **143**, 443 (1966).
- [10] S. Pal, *J. Phys. Soc. Japan* **35**, 1487 (1973).
- [11] M. Lax, Proc. of International Conference on Lattice Dynamics, Copenhagen A24, 1963.
- [12] J. Lindhard, *K. Dan. Vidensk Selsk. Mat.-Fys. Medd.* **28**, 8 (1954).
- [13] J. Hubbard, *Proc. R. Soc. A* **243**, 336 (1957).
- [14] D. J. W. Geldart, S. H. Vosko, *Can. J. Phys.* **44**, 2137 (1966).
- [15] D. L. Langreth, *Phys. Rev.* **181**, 753 (1969).
- [16] D. Pines, P. Nozières, *The Theory of Quantum Liquids*, Vol. I, 326, W. A. Benjamin Inc. 1966.
- [17] A. W. Overhauser, *Phys. Rev.* **B3**, 1888 (1971).
- [18] K. S. Singwi, M. P. Tosi, R. H. Land, A. Sjolander, *Phys. Rev.* **176**, 589 (1968).
- [19] W. A. Kamitakahara, B. N. Brockhouse, *Phys. Lett.* **29**, 639 (1969).
- [20] J. W. Lynn, H. G. Smith, R. M. Nicklow, *Phys. Rev.* **B8**, 3494 (1973).
- [21] J. R. Neighbours, G. A. Alers, *Phys. Rev.* **111**, 707 (1958).
- [22] J. Bahari, B. B. Tripathi, *Phys. Lett.* **29A**, 313 (1969).
- [23] Y. P. Varshni, P. S. Yuen, *Phys. Rev.* **164**, 895 (1967).
- [24] W. F. Giaque, P. F. Meads, *J. Am. Chem. Soc.* **63**, 1897 (1941).
- [25] T. H. Gebelle, W. F. Giaque, *J. Am. Chem. Soc.* **74**, 2368 (1952).
- [26] F. E. Hoare, B. Yates, *Proc. R. Soc. A* **240**, 42 (1957).
- [27] W. S. Corek, M. P. Garfunkl, C. B. Satterthwaite, A. Wexler, *Phys. Rev.* **98**, 1599 (1956).
- [28] H. Closs, M. M. Shukla, *Physica* **79B**, 26 (1975).
- [29] D. L. Price, K. S. Singwi, M. P. Fosi, *Phys. Rev.* **B2**, 2983 (1970).
- [30] K. Krebs, K. Holtz, *Phys. Kondens. Mater.* **15**, 87 (1972).